Supplementary Information for

Mechanism of reactant and product dissociation from the Anthrax Edema Factor: a Locally Enhanced Sampling and Steered Molecular Dynamics Study

Leandro Martínez, Thérèse E. Malliavin, Arnaud Blondel

Unité de Bioinformatique Structurale, URA CNRS 2185, Institut Pasteur, 25, rue du Dr Roux, F-75015 Paris, France.

and

Instituto de Física de São Carlos, Universidade de São Paulo. Av. Trabalhador São-carlense 400, 13566-590 São Carlos, SP, Brasil. e-mail: leandro@ifsc.usp.br

Targeted Molecular Dynamics Simulations

Auxiliary Targeted Molecular Dynamics (TMD) simulations [1] were performed to support the features of the dissociation paths observed by SMD. In TMD, the transition from a initial to a final structure is induced by applying a additional potential of the form

$$U_{TMD} = \frac{1}{2}\frac{k}{N}\Delta RMS^2$$

where $\Delta RMS = RMS(t) - RMS^*(t)$, with $RMS(t)$ being the instantaneous best-fit RMS deviation of the current coordinates from the target coordinates, and $RMS^*(t)$ evolves linearly from the initial RMSD at the first TMD step to the final RMSD at the last TMD step. k is the spring constant and N the number of targeted atoms [2]. The pace at which ΔRMS varies indicates how hard is to promote the structural transitions. A positive ΔRMS indicates that the structure is approaching less than linearly the target structure.

All simulations were performed using the equilibrated systems (described in the main manuscript Materials and Methods) as initial coordinates, using a final position from LES simulations for the ligands as target coordinates, and were 1 ns long. A constant $k = 200$ kcal mol^{-1}Å^{-2} was used, as suggested in [3]. In NAMD's TMD implementation the current coordinates are aligned to target coordinates at every step before computing the RMS in order to remove translational and rotational displacements. In our case, however, ligand dissociation is an essentially translational motion, so we needed to define as TMD atoms, apart from the ligand atoms, every atom of the protein farther than 20Å from the active site. These atoms have identical initial and final coordinates, and

dominate the best-fit at every step, such that the displacement of the ligand is preserved (because the ligand is displaced relative to these atoms). The force is significant only for ligand atoms, because the RMS of these protein atoms is almost zero at every step.

TMD simulations confirmed the general features of ligand dissociation observed in SMD runs. As shown in Figure S1, dissociation of products from 1sk6-Mg2 is harder (ΔRMSs are larger) than from 1sk6-cMg. cAMP dissociation never drags Mg^{2+} from the binding pocket, while the MgP ion dissociates with PPi when PPi dissociates from 1sk6-Mg2. The breakage of ligand-Mg^{2+} or Mg^{2+}-protein interactions was confirmed as the most important step for dissociation, as indicated by the fast and sharp ΔRMS decrease that accompanied these events, particularly in cAMP and PPi dissociations from 1sk6-Mg2 (Figure S1, (a) and (b)). The increase in the number of water molecules solvating Mg^{2+} ions is observed in 1sk6-Mg2. Solvation of products increase relative to the beginning of the simulation, and partially compensates the loss of ligand-protein interactions.

ATP dissociations induced by TMD also displayed similar features as SMD runs: Dissociation of ATP from 1k90 is harder than from 1xfv-Mg2, as indicated by ΔRMSs (Figure S2(a)). The cMg ion is tightly bound to ATP and totally protected from solvent in 1k90. Dissociation of ATP from 1K90 dragged the ion from the binding pocket (ATP-cMg interaction are maintained, Figure S2(b)), a process that is accompanied by increased Mg^{2+} solvation, as shown in Figure S2(c). The interactions of ATP with the whole environment are more strong in 1xfv-Mg2 (Figure S2(d)), but only because of interactions

with the non-central Mg^{2+} ion, which is tightly coordinated by ATP, although not to catalytic site residues (see main text). ATP dissociation from 1xfv-Mg2 didn't induce Mg^{2+} dissociation, as ATP-cMg interaction is not as strong as in 1K90.

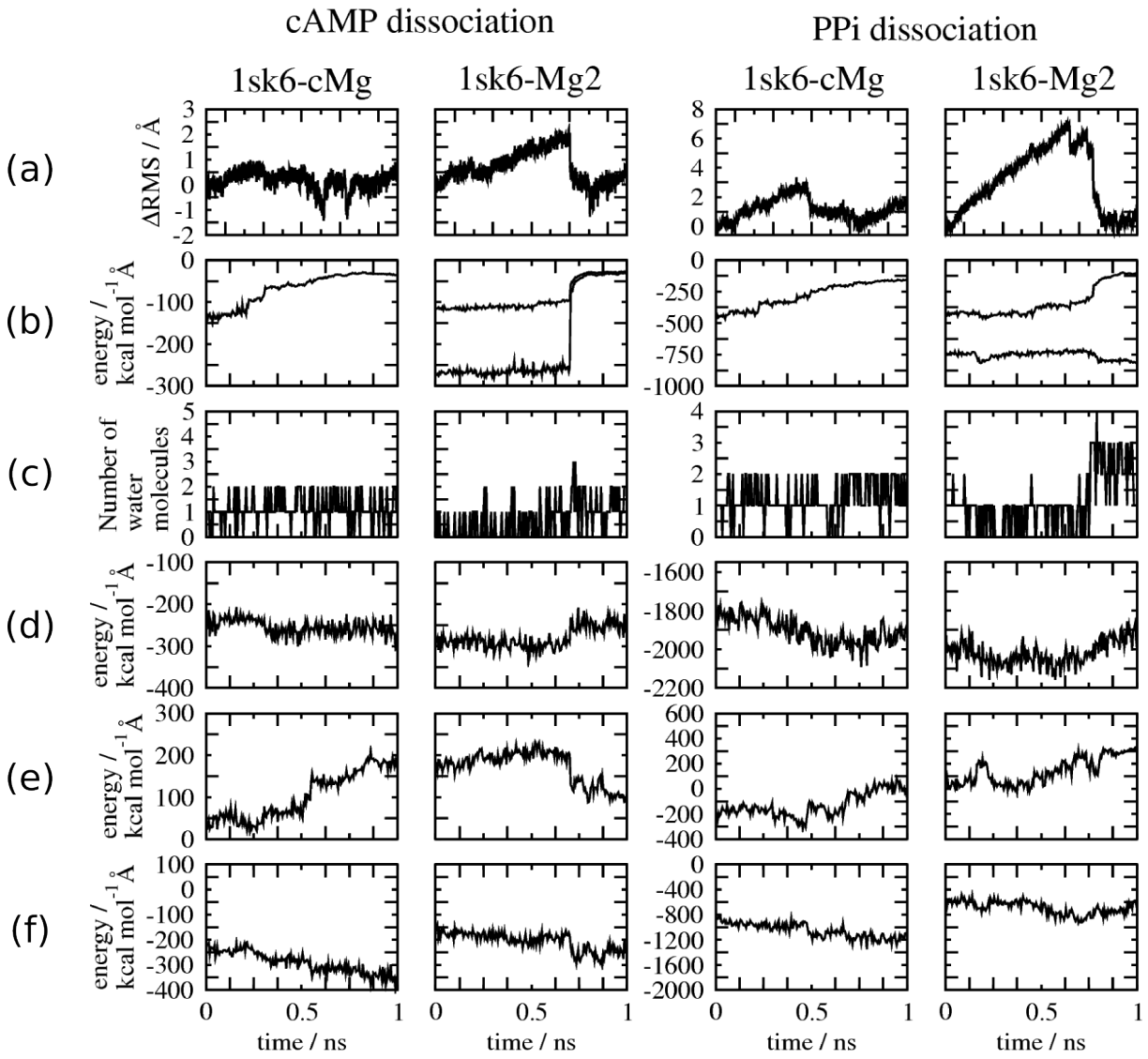

Figure S1. cAMP and PPi dissociation probed by TMD simulations: (a) ΔRMS: difference in linearly predicted (target) vs current RMS of the ligands. (b) Interaction energies of products with Mg^{2+} ions. (c) Number of water molecules having an atom closer than 2 Å from the central-Mg^{2+} ion. ATP interaction energy with (d) the whole environment (EF-Cam+water), (e) the protein and (f) water molecules.

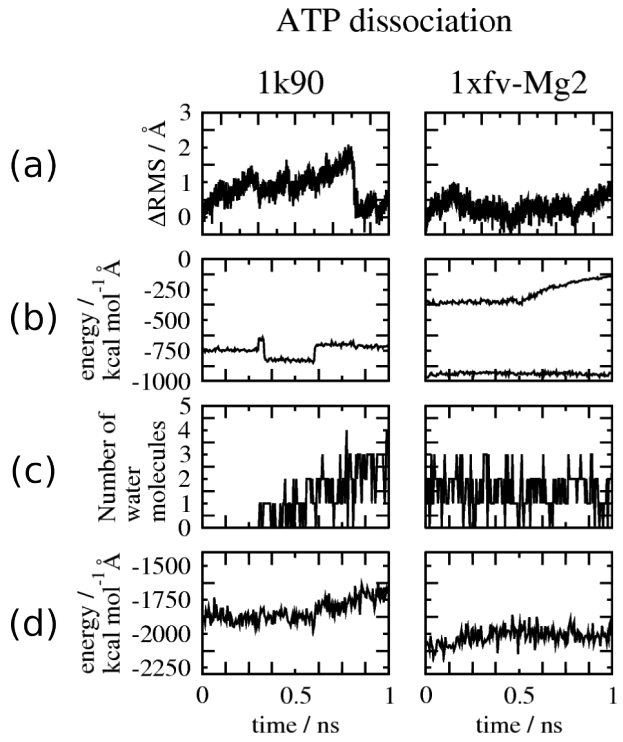

Figure S2. ATP dissociation probed by TMD simulations: (a) ΔRMS: difference in linearly predicted (target) vs current RMS of the ligands. (b) Interaction energies of ATP with Mg^{2+} ions. (c) Number of water molecules having an atom closer than 2 Å from the central-Mg^{2+} ion. ATP interaction energy with (d) the whole environment (EF-Cam+water), (e) the protein and Mg^{2+} ions (for 1xfv-Mg2 the non-central Mg^{2+} is not included) and (f) water molecules.

References

1. Chirsten M, van Gunsteren WF. On searching in, sampling of, and dynamically moving through coformational space of biomolecular sytems: A review. J Comp Chem

2008;29:157–166.

2. Phillips JC, Braun R, Wang W, Gumbart J, Tajkhorshid E, Villa E, Chipot C, Skeel RD, Kale L, Schulten K. Scalable molecular dynamics with NAMD. J Comput Chem 2005;26:1781–1802.

3. Bhandarkar M, Bhatele A, Bohm E, Brunner R, Buelens F, Chipot C, Dalke A, Dixit S, Fiorin G, Freddolino P, Grayson P, Gullingsrud J, Gursoy A, Hardy D, Harrison C, Hnin J, Humphrey W, Hurwitz D, Krawetz N, Kumar S, Kunzman D, Lee C, Mei C, Nelson M, Phillips J, Sarood O, Shinozaki A, Zheng G, Zhu F. NAMD User's Guide - Version 2.7. University of Illinois and Beckman Institute; 2010.